



ANALYTICAL MODELING OF NONLINEAR BEHAVIOR OF MASONRY INFILLS IN REINFORCED CONCRETE FRAME BUILDINGS UNDER SEISMIC ACTION

Nguyen Le Ninh^{1*}, Phan Van Hue²

Abstract: The presence of masonry infills significantly affects to the seismic response of reinforced concrete (RC) frame structures. However, in the modern seismic codes, this issue has not been specifically addressed, especially when the structures are allowed to work beyond the elastic limit. The paper introduces a nonlinear behavior model of the masonry infills that the authors have set up and it has been applied to evaluate the seismic response of RC frames designed according to modern conception when considering the interaction with the masonry infills. The results of nonlinear static analysis show that the masonry infills are likely to cause a sudden collapse of the structures, override the seismic design of the structures and undermine the efforts of the designers.

Keywords: Masonry infills, reinforced concrete frame, nonlinear static analysis, nonlinear behavior model, interaction.

Received: September 15th, 2017; revised: October 30th, 2017; accepted: November 2nd, 2017



1. Introduction

Masonry infills significantly affect to the surrounding frame under seismic actions. It has been well - known that masonry infills increase the stiffness, strength and energy-dissipation capacity... of the structural frames under lateral loads. The research results have also induced a better understanding of the behavior of infilled frames in different loading phases and then many models have been proposed, especially for elastic phase [1-4].

Nowadays, many changes have been taken place in the seismic design conception that transferred from designing for protecting the buildings to designing for protecting directly not only the human but also the social materials. It implies that the elastic limit of the structure is allowed to be exceeded during earthquakes with moderate or high intensity, without the occurrence of abrupt collapse [5]. In this situation, it is essential that the nonlinear behavior of the masonry infills and the interaction between them and the surrounding frame in different working phases under the horizontal impact should be adequately studied [6].

In the following sections, research results about the nonlinear behavior of the masonry infills and their influences on the seismic response of RC frame structures according to modern conception will be presented.



2. Modeling behavior of the reinforced concrete frame and the masonry infills

In the present study, the nonlinear static (pushover) analysis is selected for seismic performance estimation purposes of the building. With regard to the constitutive laws for the materials, the classical parabola-rectangle diagram has been adopted for the concrete under compression, and an elastic-hardening diagram has been adopted for the reinforcing steel through by [7]. The nonlinear behavior of columns and beams was described according to a lumped plasticity approach, in which the frame elements are elastic, all the nonlinearities are concentrated at the end-sections of the elastic beams, in a flexural plastic hinge that is defined by [8]. Acceptance criteria for deformation for components corresponding to the target Building Performance Levels of Collapse Prevention (CP), Life Safety (LS), and Immediate Occupancy (IO) are also given in [8]. The drift values are usually used to illustrate the overall structural response associated with various structural performance levels. The drift values of 1%, 2% and 4% corresponding to structural performance levels of IO, LS and CP were suggested by [9].

¹ Asso.Prof.Dr, Faculty of Building and Industrial Construction. National University of Civil Engineering.

² PhD student, MienTrung University of Civil Engineering.

* Corresponding author. E-mail: nguyeneninh47@gmail.com.

2.1 Model of nonlinear behavior of the masonry infills

The specialized scientific documents for nearly 70 years have introduced many models simulating the behavior of the masonry infills in the RC frame under the horizontal impact in the elastic phase. When increasing lateral loads, the behavior of the RC frame-masonry infills transfers from linear to nonlinear because of the material nonlinearities of the infill panel, the surrounding RC frame, and the panel-frame interfaces. The nonlinear effects mentioned above introduce analytical complexities which require sophisticated computational techniques to be properly considered in the modeling. These facts complicate the analysis of infilled frame and represent one of the main reasons to explain why the modern seismic codes, example TCVN 9386:2012, don't provide any specific provisions of how to consider the infill-frame interaction, although masonry infills' influence is strongly admitted on the overall response of the buildings, especially when the RC frame is allowed to work after the elastic limit [10].

In recent times, some models aimed at evaluating the hysteretic behavior of the infilled frame have been found. Among different approaches, two of those proposed by [2,11] are remarkable. These models based on the equivalent diagonal strut idea, used in linear analysis and displacement - force relations are established on the basis of experimental test results. For this reason, the accuracy and the applicability of the proposed model are limited. To resolve this existing problem, a nonlinear behavior model of the masonry infills in the RC frame has been developed by the authors based on research results of [1].

To develop the idea of the preceded authors, the proposed model has still been based on the equivalent diagonal strut model but the equivalent strut's width w_m that was suggested by [1] varies during the bearing process (Fig. 1). Whereby, the equivalent diagonal strut's width is determined according to the following expression [1,5]:

$$w_m = e^{m(1-n)} w_{m0} \quad (1)$$

where m is the factor that depends on the characteristics of the masonry infills ($m = 2$ for clay brick masonry infills, $m = 3.6$ for aerated autoclaved concrete masonry infills); $n = V/V_{mu}$ is the ratio of the horizontal force and the ultimate horizontal strength; w_{m0} is the basic width of the equivalent strut at the time the masonry infills hypothetically are not enough strength and stiffness to participate in bearing with the surrounding frame:

$$w_{m0} = \frac{d_m}{\lambda_h h + \lambda_l l + k} \quad (2)$$

In the above formulation, λ_h and λ_l are the parameters of the lengths of contact z_h , z_l between the infill and column, beam given by the following expressions:

$$\lambda_h = \sqrt[4]{\frac{E_m t_m l_m}{4 E_c I_c h_m^2}} \quad \text{and} \quad \lambda_l = \sqrt[4]{\frac{E_m t_m h_m}{4 E_c I_b l_m^2}} \quad (3)$$

where E_m and E_c are the elastic modulus of the masonry infill and concrete, respectively; l and h are the length of beam and the height of column, measured between the centerlines of the columns and the beams, respectively; l_m , h_m , d_m and t_m are the length, the height, the diagonal length and the thickness of the infill, respectively; I_b , I_c are the moment of inertia of the beam and the column, respectively; k is the factor that depends on the characteristics of the masonry infills ($k = 3.5$ for clay brick masonry infills, $k = 20$ for aerated autoclaved concrete masonry infills).

In this model (Fig. 2), the nonlinear behavior of the panel infills in the frame is modeled by the equivalent diagonal strut with a single plastic hinge in the middle. The form of the proposed model is similar to the ones of models proposed by [2,11]. The relationship between the shear force V_m and the horizontal displacement of masonry infill Δ_m is composed by four phases, with the acceptance criteria for deformation of the masonry infill materials. The first phase represents the linear behavior of the infill that is depicted by the straight line between point A (unloaded situation) and B (the effective yield point), with the stiffness K_{my} . According to [1], this phase ends when $n = 0.6$. The second phase (segment BC) represents the nonlinear behavior like

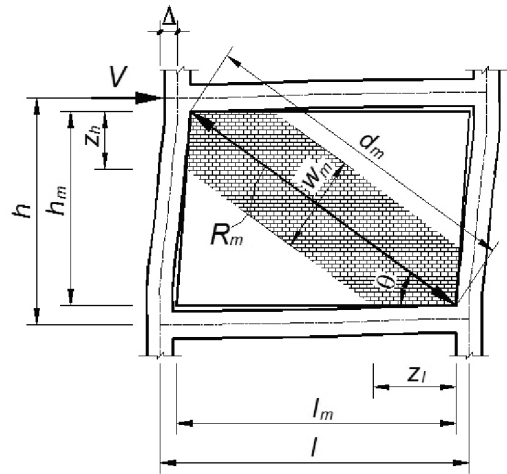


Figure 1. The equivalent diagonal strut model

the phenomenon of deformation hardening, with the stiffness $K_{mu} = \beta K_{my}$ is a fraction of the elastic stiffness (β is the stiffness ratio between K_{mu} and K_{my}). According to [1] this phase ends when $n = 1.0$. At point C, the ordinate denotes the ultimate strength of infill and the abscissa indicates the deformation when the strength starts to decrease seriously (segment CD). Due to the brittle failure of the masonry infill, the acceptance criteria for deformation for the infill corresponding to the target building performance levels of LS and CP as shown in Fig. 2 nearly coincide. The third phase is the post-capping degrading phase, which runs from the maximum strength to the residual strength. Its stiffness depends on the elastic stiffness, and is defined by means of the parameter γ as $K_{mr} = -\gamma \cdot K_{my}$. It has been suggested that γ should be within the range of values between 0.005 and 0.1, although the upper value corresponds to very brittle infill. After point D, the masonry infill is characterized by the constant residual strength V_{mr} to enhance the numerical stability of the analysis. The residual strength of masonry infill can be ignored by prolonging the segment CD until a zero residual strength (dashed line in Fig. 2), corresponds to the displacement Δ_{mp} . Thus, the calculation and the assessment of infills are carried out only at the two target building performance levels of IO and LS, in accordance with the provisions of the current standards of many countries [8,9,12].

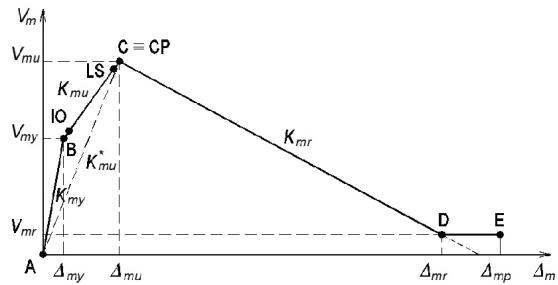


Figure 2. The Force-Displacement relationship for the equivalent strut model

2.2 Define the lateral stiffness parameters of the masonry infills

Generally, the lateral stiffness of the masonry infills at different working phases is determined by the following expression [1]:

$$K_m = \frac{e^{m(1-n)} w_{m0} t_m E_m \cos^2 \theta}{d_m} \quad (4)$$

where w_{m0} is the basic width of the equivalent strut that is defined by the expression (2); λ_h and λ_l are given by the expression (3); θ is the slope angle of the panel's diagonal to the horizontal.

- At the time the masonry infill is yields, $n = 0.6$:

$$K_{my} = \frac{e^{0.4m} w_{m0} t_m E_m \cos^2 \theta}{d_m} \quad (5)$$

- At the time the masonry infill reaches the ultimate strength, $n = 1.0$:

$$K_{mu}^* = \frac{w_{m0} t_m E_m \cos^2 \theta}{d_m} = \frac{K_{my}}{e^{0.4m}} \quad (6)$$

2.3 Define the strength parameters of the masonry infills

Based on the extensive investigations in last seven decades [3,13,14], four different failure models of the infill panels viz., bed-joint sliding shear failure, cracking due to diagonal tension, compression failure of diagonal strut, and corner crushing of infills, have been identified. Several models have been proposed for evaluating strength of the masonry infills in these failure models. In the above failure models, bed-joint sliding shear failure and compression failure of diagonal strut are the most commonly identified failure models.

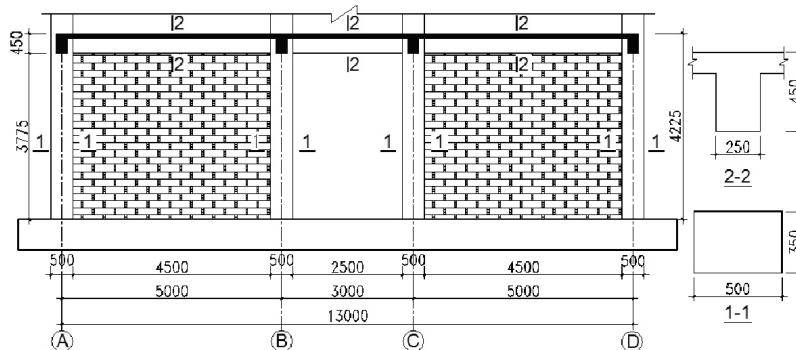


Figure 3. Cross section of considered frame (1st floor)

The choice of method for determining the strength of the infills corresponding to each of their different failure forms is a very important factor in order to determine the strength of the infills in accordance with the purpose and scope of this study. The criteria used to select the strength of the infills for the nonlinear behavior of the infills are as follows:

- The parameters used to determine the strength of the infills should be compliant with the current Vietnamese technical standards;
- The infills are constructed by conventional clay brick masonry in Vietnam in the RC frame according to the current technical provisions.

As is well-known, the strength of the infills depends on the geometrical and mechanical properties of the materials as well as the infilled frame structure, therefore the infilled frame structure shown in Fig. 3 has been considered to choose comparatively a suitable calculated method.

The 1st floor cross section of considered frame of the 10-storey RC frame building is represented in Fig. 3. The frame is constructed of the B25 grade of concrete. The beams at the outermost span of the frame (AB and CD spans) are infilled by 200mm thickness masonry that is constructed of plastic laminating burnt clay bricks M75 and cement mortar M75. The physico-mechanical properties of the masonry infills and the materials constituting the RC frame are defined in accordance with TCVN 5573:2011 [15] and TCVN 5574:2012 [16].

In the following section, the strength of the masonry infills at the characteristic points B, C, D and E in the behavior model in Fig. 2 will be shown how to determine according to the collective research results that have been realized about this issue.

2.3.1 The ultimate strength of masonry infill V_{mu}

The ultimate strength of masonry infill, V_{mu} , is the minimum value of strengths in the bed - joint sliding shear failure model, V_{ms} , and the compression failure of diagonal strut, V_{mc} :

$$V_{mu} = \min(V_{ms}, V_{mc}) \quad (7)$$

Over the past 70 years, many researchers have proposed different models for determining the strength of masonry infills in the sliding shear failure mode and compression failure of diagonal strut. Figs. 4 and 5 summarize the results of calculating the strength of masonry infills in accordance with the different approaches in sliding shear failure and compression failure of diagonal strut.

In Fig. 4, the results of strength of infill in the sliding shear failure model are calculated according to different approaches that are in line with the chosen criteria: [17], [14], [3] with $\mu = 0.7$ and $\mu = 0.3$; [8,9,13]; [18], [12], [9]; the method is proposed by authors.

In Fig. 5, the results of strength of infill in the compression failure of diagonal strut are given by different approaches that are in line with the chosen criteria: [3,17], [14], [18], [12], [13], [4], [8].

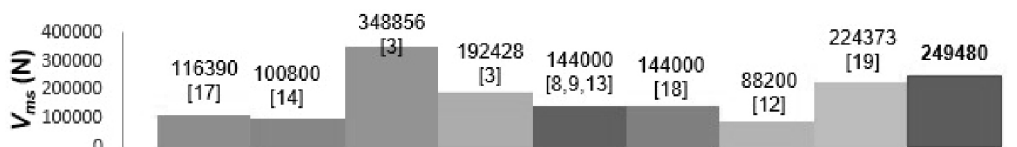


Figure 4. Comparison of the strengths of infill in the sliding shear failure mode in accordance with different approaches

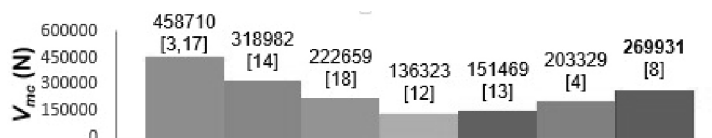


Figure 5. Comparison of the strengths of infill in the compression failure of diagonal strut in accordance with different approaches

The results in Figs. 4 and 5 show that there is a significant difference between values of strength of the infill in accordance with the different approaches. Based on the analysis of the advantages and disadvantages of each method as well as the results obtained under the current conditions of application in Vietnam, the models determining the ultimate strength of the infill are the ones proposed by the following researchers:



a) The ultimate strength of masonry infills in the sliding shear failure model, V_{ms} , which proposed by the authors based on the bed-joint shear strength of the masonry unbraced shall be calculated in accordance with TCVN 5573:2011 [15]:

$$V_{ms} = \frac{f_{bs} t_m l_m}{1 - 0.72 n_1 \mu t g \theta} \quad (8)$$

where f_{bs} is the bond shear strength between brick and mortar; μ is the coefficient of friction for mortar - brick interfaces; $n_1 = 1$ for solid brick masonry, 0.5 for hollow brick masonry.

Expression (8) is established with the assumption that the masonry infill carries no vertical load due to gravity effects, the clamping force across the potential sliding surface will be due only to the vertical component of the diagonal compression force in infill panel.

b) The ultimate strength of infill in the compression failure of diagonal strut is recommended by [8]:

$$V_{mc} = f_{mc} \frac{h_m}{3} t_m \cos \theta \quad (9)$$

where f_{mc} is the compressive strength of the masonry.

2.3.2 The strength of the masonry infill at yielding V_{my}

In Fig. 6, the results of strength of infill with the same parameters as those in the previous section at the beginning of yielding are calculated according to different approaches that are in line with the chosen criteria: [1], [14], [20], [2], [12], [4]. Based on the analysis of the calculated models, the equation proposed by [1] was chosen because of its simplicity as well as the average calculated value compared to other approaches:

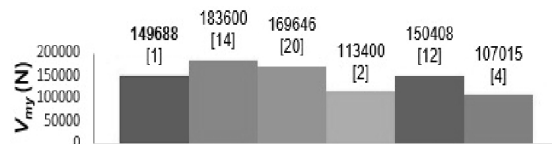


Figure 6. Comparison strength of the infill at the beginning of yielding according to different approaches

$$V_{my} = 0.6 V_{mu} \quad (10)$$

2.3.3 The residual strength of the masonry infill V_{mr}

The residual strength of the masonry infill V_{mr} is within the following limit [6]:

$$0 \leq V_{mr} \leq 0.1 V_{my} \quad (11)$$

2.4 Define the displacement parameters of the masonry infills

The displacement of the masonry infill when it reaches the ultimate strength:

$$\Delta_{mu} = \frac{V_{mu}}{K_{mu}^*} \quad (12)$$

The displacement of the masonry infill at the first yield point:

$$\Delta_{my} = \frac{V_{my}}{K_{my}} \quad (13)$$

The displacement of the masonry infill corresponds to residual strength V_{mr} :

$$\Delta_{mr} = \Delta_{mu} + \frac{V_{mr} - V_{mu}}{K_{mr}} \quad (14)$$

Thus, this model that has established for nonlinear behavior of the masonry infills is based on the experimental and analytical research results of [1] about the lateral stiffness and the strength at the beginning of yielding of the infills. Simultaneously, it is also based on the results of theoretical and empirical research about the strength of different infills in RC frames corresponding to each type of failure models gained by many researchers in the world. The parameters that used to determine the strength of infills are in accordance with the current Vietnamese technical standards. This model has reflected the actual behavior of the masonry infills in the various stages under the effect of horizontal loads. Thus, the model can be used to evaluate the influence of the infills on the response of RC frame structures under the effect of this loads.



3. Nonlinear static analysis of the reinforced concrete frame structure designed according to TCVN 9386:2012

3.1 Structural characteristics of the case study building

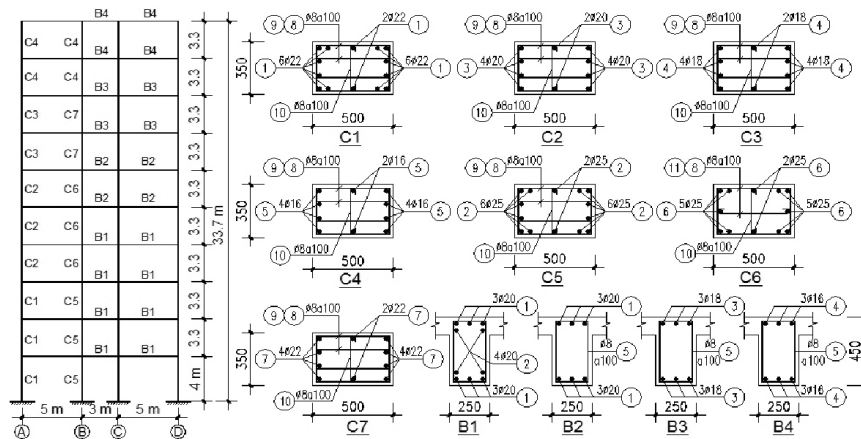


Figure 7. The global geometry and reinforcements of the frame components

This numerical example is performed to evaluate the effect of the masonry infill on the nonlinear response of the RC frame designed according to TCVN 9386:2012 [10] under the seismic action. The frame is designed for ductility classes medium (DCM), the important factor $\gamma_i = 1.25$, built at the area with the reference peak ground acceleration $a_{gR} = 0.1097g$, on the type D ground. The global geometry and the basic dimensions of the frame are given in Fig. 7. The frame is constructed of the B25 grade of concrete, the longitudinal reinforcement of beams and columns of group AIII, the transversal reinforcement of group AI. On the beams at the outermost span of the frame (AB and CD spans) are infilled by 200mm thickness masonry walls that are constructed of plastic laminating burnt clay bricks M75 and cement mortar M75. The physico-mechanical properties of the masonry infills and the materials constituting the RC frame are defined in accordance with TCVN 5573:2011 [15] and TCVN 5574:2012 [16]. The values of vertical load that act on the beams at each floor in the seismic design situation, $g + \psi_2 q$, are alternately given by 22.1 kN/m (the side spans of the transverse beam); 11.8 kN/m (the middle span of the transverse beam); 15 kN/m (the longitudinal boundary beams) and 19.8 kN/m (the longitudinal middle beams).

3.2 The response of the RC frame in the case of not considering the interaction between frames and masonry infills

The RC frame structure is designed according to TCVN 9386:2012 under the seismic action. In the case of not considering the interaction between the frame and the masonry infills (bare frame), the design results for the reinforcements of the frame components are shown in Fig. 7. The nonlinear static analysis is carried out by SAP2000, with the lateral force acting as forced displacements. It is assumed that flexural deformations control the nonlinear behavior of columns and beams. The analysis is performed until the frame reaches the target displacement $\Delta = 1.348$ m. Fig. 8a is the diagram of flexural plastic hinges that appear in the frame at the time of taking place a hypothetical collapse. This figure shows that, without considering the interaction between frame and masonry infills, the plastic failure mechanisms are expectedly happened with flexural plastic hinges first appearing in the beams and then in the columns.

The solid line in Fig. 9 is the capacity curve that represents the nonlinear behavior of the bare frame. This curve shows that the linear deformation of the frame ends at 10th step ($V = 466.297$ kN, $\Delta = 0.126$ m).

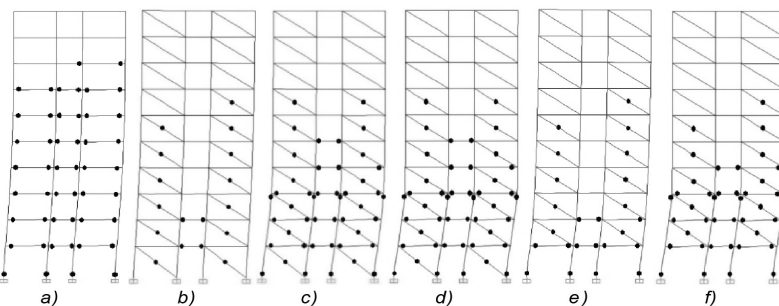


Figure 8. Plastic deformation diagrams of the frame and masonry infills

a) bare frame; b), c), d) frame with infills of all floors; e), f) infilled frame without infills on the 1st floor

The lateral stiffness of the frame in this stage K_{bf} = 3700 kN/m. The maximum base shear force V = 726.13 kN and the horizontal displacement respectively Δ = 0.559 m at 40th step. After this point, the lateral stiffness of the frame almost linearly decreases. At the end of pushover progression at step 97, the base shear force attains the value of V = 666.52 kN.

3.3 The response of the frame in the case of considering the interaction between frames and masonry infills

a) In case of having masonry infills in the 1st and 3rd side spans of the all floors

In this case, to establish the nonlinear behavior model of the masonry infill, the parameters related to the stiffness of the masonry infill types (w_{m0} , K_{my} , K_{mu}^* and K_{mr}) are given in Table 1. The parameters related to the strengths as well as the displacement values of the masonry infills defined by the expressions from (12) to (14) are given in Fig. 10.

Table 1. The stiffness parameters of the masonry infills

Parameters	w_{m0} (mm)	w_m (mm)	K_{mu}^* (N/mm)	K_{my} (N/mm)	K_{mr} (N/mm)
1 st floor	609	1356	17046	37937	-2656
2 nd ÷ 10 th floors	575	1279	21555	47973	-3358

The results of the nonlinear static analysis show that, starting at the third loading step until the sixth loading step, the masonry infills in turn from the first floor to the sixth one are deformed at different degrees (LS and IO states). At the 8th step (V = 881.24 kN, Δ = 0.113 m), the masonry infills of the three bottom floors are collapsed together, leading to the appearance of yielding at the ends of the beams in the middle span of the 1st floor and the 2nd floor while the masonry infills in the upper floors continue being plastically deformed in different degrees (Fig. 8b). The plastic deformation at the bases of the first floor columns begins at the 10th step (V = 954.302 kN and Δ = 0.140 m) and continues increasing until 15th step when all the bases of the first floor columns are yielded. Unlike bare frame, the upper butts of columns on the third floor are yielded at 39th step (V = 793.077kN and Δ = 0.463 m) (Fig. 8c). The infilled frame gradually approaches the collapse state in accordance with soft story collapse mechanism nearly while in all the ends of the beams in the 3rd floor only appear nonlinear deformations at LS state, in several ends of the beams in the 4th and 5th floors only appear nonlinear deformations at IO state, the masonry infills in the 5th, 6th and 7th floors are plastically deformed at IO and LS states as 10th step and total beams, columns and infills in the upper floors are remain in the elastic limit. Until the target displacement reaches Δ = 1.345 m, the plastic deformations are almost focused on the bases of columns on the foundation surface and the butts of columns on 3rd floor (Fig. 8d).

The dashed line in Fig. 9 is the capacity curve of the frame with masonry infills at two side spans of all floors. This curve has a completely different form from the capacity curve of the bare frame (solid line). In the first stage until the base shear force reaches to V = 881.24 kN and Δ = 0.113 m at the eighth step, the structural system behaves almost linearly with the lateral stiffness of K_{if} = 7800 kN/m. When the base shear force reaches the maximum value of V = 983.299 kN and Δ = 0.189 m at 15th step, the stiffness of structural system is suddenly decreased and varies unequally, consistent with different failure states of the masonry infills on the frame's height. At 70th step, when V = 715.8 kN corresponding to Δ = 0.804 m, the overall capacity of bearing force of the composite infilled frame is nearly transferred to bottom floors. The composite structural system is declined its stiffness near linear but with a greater slope than the bare frame.

b) In case of not having masonry infills in the 1st and 3rd side spans of the first floor

In this case, the capacity curve of the composite structural system (dashed-dot line) in Fig. 9 has some important differences compared to the two above cases:

- Compared to the case of being infilled the whole first floor, the base shear force is not declined suddenly and the decline of bearing force capacity after elasticity is more regular. The linear elasticity phase

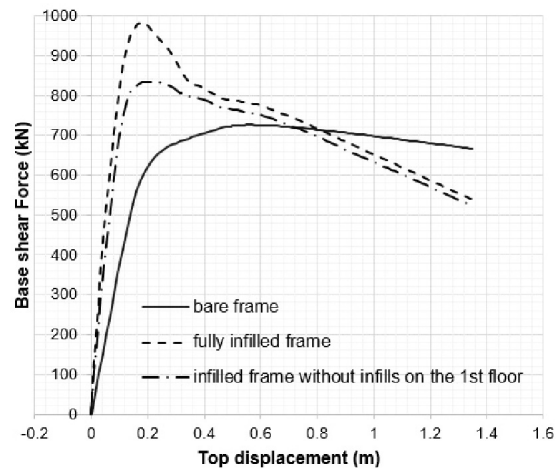


Figure 9. Capacity curves

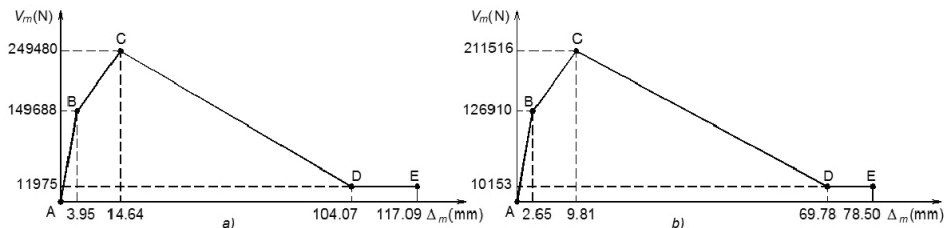


Figure 10. The Force-Displacement relationships for the equivalent strut model of the masonry infill
a) 1st floor; b) 2nd to 10th floors

ends much earlier compared to fully infilled frame and closer to bare frame.

- The moment of transferring the bearing force capacity of the infilled frame to the frames in bottom floors ($V = 718.607$ kN; $\Delta = 0.726$ m) is earlier than fully infilled frames.

Therefore, when the first floor is empty, the response of the composite structural system before and after transferring is much less than that of being fully infilled, the bearing force capacity is reduced more drastically than cases of bare frame and fully infilled frame. The analysis results show that, the flexural plastic hinges appearing at the column bases of the 1st floor are much earlier (from 8th step to 10th step) than fully infilled frame (Fig. 8e). When the target displacement reaches to $\Delta = 1.346$ m (107th step), the base shear force of infilled frame with the first empty floor ($V = 523.808$ kN) is nearly 1.3 times smaller than the bare frame. At this time, all the column bases on the foundation surface and the column butts on the 3rd floor are yielded like the fully infilled frame but at an earlier time (Fig. 8f).

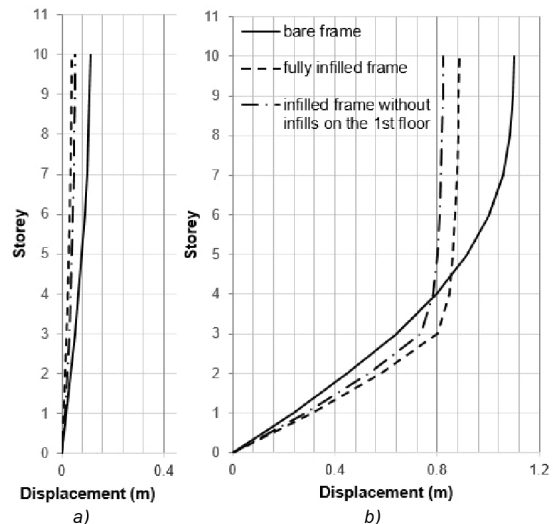


Figure 11. Horizontal displacements of the frame structures

Figs 11a and 11b show that there is a great difference between the horizontal displacements of the frame structures in three cases at different stages: linearly when $V = 415.243$ kN (Fig. 11a) and after elasticity when $V = 689.049$ kN (Fig. 11b). In the stage of post-elastic working, the deformation of the infilled frame is almost concentrated in columns of the lowest floors, while the deformations of the components on upper floors are almost unchanged. The risk of sudden collapse of the bottom floors (soft story collapse mechanisms) is significant, especially when there is no infills in the first floor (Fig. 11b).



4. Conclusions

This paper has proposed the nonlinear behavior model of the masonry infills and it has been applied to evaluate the seismic response of RC frames designed according to TCVN 9386:2012 when considering the interaction with the masonry infills. The proposed model has still been based on the equivalent diagonal strut model but the equivalent strut's width varies during the bearing process. The analytical results show that the capacity curves and the behavior of infilled frames generally appropriate with experimental data and analytical results by other researchers. This, however, requires a fine calibration of the model that attains a higher reliability in the prediction the response of infilled frames.

The results of nonlinear static analysis show that the masonry infills in the RC frames radically change the response of the RC frame structures designed according to TCVN 9386:2012:

- The failure mechanisms of the frames change from beam-sway mechanisms (strong column/weak beam) to soft story mechanisms (weak column/strong beam).

- In the case of considering the interaction between the frames and the infills, after the peak base shear force reaches, the infilled frame structure has suddenly reduced its strength and stiffness due to the brittle failure of the panels infilled of bottom floors. After this stage, the whole deformation of the composite structure will be almost concentrated on columns of bottom floors.



- Infill panels of bottom floors are collapsed earliest while the ones of the upper floors are almost not deformed. The response of the present frame is not the same as that of the bare frame. The soft story collapse mechanisms occur, especially when there are not any infills of bottom floor, the collapse of the composite structure will occur earlier and more dangerous compared to fully infilled frame.

- The bending stiffness of the beams in the infilled frames is larger than the one in the bare frame.

Thus, the presence of masonry infills in the RC frame structures designed according to TCVN 9386:2012 has completely changed the intention of the designers. This is a very dangerous situation for buildings designed to withstand the seismic action currently. Therefore, in order to ensure the safety of RC frame structures, it is necessary to consider and adjust some contents in the capacity design of the RC frame structures defined in TCVN 9386:2012.

References

1. Ninh N.L. (1980), *Analysis and Design of Masonry Infilled Multistory Reinforced Concrete Frame Structures for Cyclic Lateral Loads*, Doctoral thesis, Bucharest Institute of Construction, Romania (in Romanian).
2. Panagiotakos T.B., Fardis M.N. (1996), "Seismic response of infilled RC frame structures", *Proceedings of the eleventh world conference on earthquake engineering*, Mexico.
3. Paulay T., Priestley M.J.N. (1992), *Seismic design of reinforced concrete and masonry buildings*, A Wiley Interscience Publication, New York.
4. Tucker C.J. (2007), *Predicting the in-plane capacity of masonry infilled frames*, PhD Thesis, Faculty of the Graduate School, Tennessee Technological University, USA.
5. Ninh N.L. (2007), *Earthquake and Seismic Design of Structures*, Construction Publishing House, Ha Noi (in Vietnamese).
6. Uva G., Raffaele D., Porco F., Fiore A. (2012), "On the role of equivalent strut models in the seismic assessment of infilled RC buildings", *Engineering Structures*, (42):83-94.
7. EN 1992-1-1:2004 (2004), *Eurocode 2: Design of concrete structures-Part 1-1: General rules and rules for buildings*, European Commission for Standardization, Brussels.
8. ASCE/SEI 41-13 (2014), *Seismic evaluation and retrofit of existing buildings*, American Society of Civil Engineers, Virginia, USA.
9. FEMA 356 (ASCE 2000) (2000), *Prestandard and commentary for the seismic rehabilitation of buildings*, Federal Emergency Management Agency, Washington, USA.
10. TCVN 9386:2012, *Design of structures for earthquake resistances*, Ha Noi (in Vietnamese).
11. Bertoldi S.H., Decanini L.D., Gavarini C. (1993), "Infilled frames subjected to seismic action - a simplified modeling: experimental and numerical comparison", *Proc. of the 6th National Conference ANIDIS*, Perugia, 2:815-824 [in Italian].
12. FEMA 306 (1998), *Evaluation of earthquake damaged concrete and masonry wall buildings - Basic procedures manual*, Federal Emergency Management Agency, Washington, USA.
13. Al-Chaar G. (2002), *Evaluating strength and stiffness of unreinforced masonry infill structures*, Technical Report ERDC/CERL TR-02-1, U.S. Army Corps of Engineers.
14. Smith B.S., Coull A. (1991), *Tall building structures: Analysis and design*, A Wiley Interscience Publication, New York.
15. TCVN 5573:2011, *Masonry and reinforced masonry structures-Design standard*, Ha Noi (in Vietnamese).
16. TCVN 5574:2012, *Concrete and reinforced concrete structures-Design standard*, Ha Noi (in Vietnamese).
17. Rosenblueth E. (1980), *Design of Earthquake Resistant Structures*, John Wiley & Sons Inc, New York.
18. Galanti F.M.B., Scarpas A., Vrouwenvelder A.C.W.M. (1998), "Calibration of a capacity design procedure for infilled reinforced concrete frames", *Proc. of the 11th European Conference on Earthquake Engineering*, France, A.A. Balkema Publishers, Rotterdam, 1-10.
19. TMS 402-13/ ACI 530-13/ ASCE 5-13 (2013), *Building Code Requirements for Masonry Structures* and TMS 602-13/ ACI 530.1-13/ ASCE 6-13 (2013), *Specification for Masonry Structures*, Masonry Standards Joint Committee.
20. Priestley M.J.N., Calvi G.M. (1991), "Towards a capacity-design assessment procedure for reinforced concrete frames", *Earthquake Spectra*, 7(3):413-437.